Desalination and Water Treatment
www.deswater.com

doi: 10.5004/dwt.2022.28038

247 (2022) 144–155
January

Potentiality of unfertilized mango flowering buds for removing Cd, Cu, and Pb from aqueous solutions

Ahmed Abdo

Environmental Engineering Department, Faculty of Engineering, Zagazig University, Zagazig 44519, Egypt, email: aahusin@eng.zu.edu.eg

Received 2 May 2021; Accepted 29 November 2021

ABSTRACT

Heavy metals (Cd, Cu, Pb) adsorption capacity experiments with a novel adsorbent Unfertilized Mango Flowering Buds (UMFB) were investigated in a batch scale studies at different constraints to obtain prime conditions of adsorption dose, initial metals concentration, contact time, pH, and temperature. The results showed that increasing the dosage of UMFB to 6 g/L enhanced the removal efficiency of Cd, Cu, and Pb to 82.46%, 65.74% and 74.99% respectively. The ideal biosorption limits were seen at pH 5–6 with efficiency up to 80.77%, 69.41% and 71.05% for Cd, Cu, and Pb respectively. The capacities of heavy metals removal, on the other hand, were found to be 14.51 mg/g of UMFB for Cd, 12.57 mg/g of UMFB for Cu, and 12.98 mg/g of UMFB for Pb. The ideal estimations of contact time were found at 120 min. The respective removal rates of Cd, Cu and Pb were 82.77%, 73.26%, and 79.64% while the respective adsorption capacities of Cd, Cu and Pb were 14.44, 12.65 and 13.07 mg/g. The highest accepted initial metal concentration that can achieve acceptable metal removal was not the same for the all tested metals: 100, 50, and 200 g/L for Cd, Cu, and Pb respectively. The results showed that the most suitable sorption temperature is at 40°C with a removal rate of 80.90% and 75.75% for Cd and Pb respectively, and at 60°C for Cu with a removal rate of 77.32%. The coexisting ions weakened the removal efficiency of Cd due to the intense competition for adsorption sites. Characterization of the UMFB has been conducted by scanning electron microscopic (SEM) images, before and after loaded of heavy metals, showed significant changes in the surface morphology, indicating the adsorption process had taken place. Fourier transform infrared spectroscopy (FTIR) indicates the organic functional groups which might be involved in the adsorption of heavy metals. Both pseudo-first and second-order models were used to evaluate the adsorption mechanism of different metals. It was found that information fitting best to pseudo-second-order model since the R^2 was almost equal to unity. The Cd, Cu, and Pb adsorption behavior on UMFB was a chemical homogeneous process fitting the Langmuir model ($R^2 \geq 0.98$) better than Freundlich one.

Keywords: Adsorption; Heavy metals; Low-cost adsorbents; Unfertilized mango flowering buds; Isotherms; Kinetics

1. Introduction

Egypt is a developing country experiencing enormous growth in manufacturing including petroleum refining, pulp and paper industries, textiles, paints and dyes, pharmaceuticals, fertilizer, metal plating, tanneries, ceramic and glass, steel, and mineral processing industries. Industrialization leads to urbanization by creating economic growth and jobs that draw people to cities, increasing the urban share of the total population. Due to rapid industrialization and urbanization, the levels of industrial pollution have been steadily rising [1]. Among the numerous classes of pollution, one routinely found in waters

and wastewaters is heavy metals pollution [2,3]. Heavy metals are easily transported and accumulated in the aquatic organisms as toxic compounds [4]. Unlike organic pollutants, heavy metals, such as Cd, Cu, and Pb, are not biodegradable and, at low levels, they become highly harmful to animals and humans' health even at trace levels [5,6]. Table 1 summarizes the characteristics of Cd, Cu, and Pb and shows the maximum allowable contaminant level according to both the World Health Organization (WHO) [7,8] and the Egyptian Ministry of Health and Population (MOHP, Decree No. 458, 2007) [9]. An estimated 80% of all industrial and municipal wastewater in the developing world is released to the environment without any prior treatment [10]. Also, many treatment techniques used in the developing world, such as chlorination and solar disinfection, are ineffective in removing heavy metals [11].

Based on the foregoing, the need for efficient, fast, reliable and inexpensive methods to remove heavy metals from wastewater is necessary for providing safe drinking water and for preventing environmental pollution. Various methods have been studied and used for the removal of heavy metals including precipitation, coagulation, electrocoagulation, membrane filtration, microbial remediation, reverse osmosis, electro dialysis, ultrafiltration, and adsorption [12,13]. Adsorption is a well-known phenomenon in treating water by removing heavy metals. Adsorbents can be classified into the following kinds: natural materials (like sawdust), treated natural materials (like activated carbons), manufactured materials (like polymeric resins), agricultural solid wastes (like fly ash), and biosorbents (like bacterial biomass) [14]. Activated carbon adsorption has been developed and tested and it can achieve high removal efficiencies for heavy metals, so it is currently being explored for use in many countries [15,16]. However, the high capital and regeneration cost of the activated carbon restrict the widespread use applications for the removal of metals [14]. Of all the methods of wastewater treatment, adsorption with agricultural waste is the most trusted one for removing heavy metals due to its cost effectiveness, availability and reliable metal removal efficiency [17]. Although, many agricultural wastes have been studied and used to remove heavy metals from metal-contaminated wastewater, there is still a lack of data regarding the possibility using of a number of cheap adsorbents prepared from agricultural wastes such as unfertilized mango flowering buds (UMFB).

Mango is a stone fruit produced from numerous species of tropical trees belonging to the flowering plant genus "Mangifera". Egypt's weather and soil are known to be a proper atmosphere for cultivating mangoes. The main governorates producing mango in Egypt include Sharkia, Ismailia, Giza, Fayoum, Qena and Beheira. Some of mango flowering buds cannot get fertilized and become useless. So, the aim of this research is to assess the ability of UMFB as an innovative and inexpensive adsorbent to remove the heavy metal ions (Cd, Cu, and Pb) from aqueous solutions. The hypothesis of this study is that using of UMFB as an adsorbent affects positively the removal of heavy metals from aqueous solutions. Several materials have been evaluated for the removal of heavy metals, but to the best of the researcher's knowledge, UMFB has not been traced yet. The present study is undertaken with the following specific objectives: to examine the performance and effectiveness of UMFB in removing Cd, Cu, and Pb ions by adsorption from aqueous solution, to determine the effect of operational parameters (such as adsorption dose, initial metals concentration, time of contact, pH, and temperature) on the adsorption capacity of the UMFB, to analyze the effect of coexisting ions on the removal efficiency of the UMFB, to study the applicability of the Langmuir and Freundlich isotherms, to study the effect of biosorption kinetics, to characterize the UMFB adsorbent by Fourier transform infrared (FTIR) spectroscopy and to study the structure of the UMFB using scanning electron microscopy (SEM).

2. Material and methods

2.1. Absorbent preparation and treatment

In this study Mango biomass was collected from orchids of Salhia (Sharkia, Egypt). The collected biomass was rinsed with 1% HCl, and flushed afterward with distilled water to remove any material clinging to buds. The biomass was dried by the heat of the sun for two weeks. The buds were removed and further dried by the sun for another two weeks and then rinsed again in distilled water. After that, the biomass was located in an oven at 70°C for 48 h to get an oven-dry weight. The biomass has been finely beaten, grinded, and then sieved through 100 and 200 mesh (Standard Sieves Dual Manufacturing Co., USA) for getting uniform size distribution. Grinded

Table 1
Characteristics of the studied heavy metals (Cd, Cu, and Pb)

Heavy metal	Human health effects	Common sources	Maximum contaminant level	
			MOHP	WHO
Cd	Kidney damage Carcinogenic	Various chemical industries Contamination from fertilizers	0.005 mg/L	0.003 mg/L
Cu	Gastrointestinal issues Liver or kidney damage	Household plumbing systems Corrosion of pipes and fittings	1.0 mg/L	2.00 mg/L
Pb	Kidney damage Reduced neural development	Lead-based products Corrosion of pipes and fittings	0.05 mg/L	0.01 mg/L

biomass was further washed with distilled water till the color of washing water became clean enough to get rid of lighter materials and other impurities.

2.2. Heavy metals

All the chemicals used are of analytical grade (AR). The heavy metals stock solutions of 1,000 mg/L were prepared by dissolving cadmium chloride monohydrate ($CdCl_2 \cdot H_2O$), copper(II) chloride($CuCl_2$), and lead(II) acetate trihydrate ($C_4H_6O_4Pb \cdot 3H_2O$) in distilled water. The actual concentration of all metal solutions was measured and then diluted as required to obtain standard solutions. NaOH (0.1 M) and HCl (0.1 M) solutions were used to adjust the pH of the heavy metal solutions.

2.3. Batch experiments procedure

The batch experiments were conducted in 50 mL bottles. The amount of adsorbent was added to 20 mL of aqueous solutions, and then mixed in a water bath mechanical shaker at 30°C. The treated solution is finally filtered before analysis. The present study aimed to establish the optimum conditions for Cd, Cu, and Pb adsorption. This involved the effects of adsorbent dosage (1.0–10.0 g/L), pH (4–9), contact time (30–240 min), initial metals concentration (10–200 mg/L) and temperature (20°C–60°C). All experiments were tested in triplicate, in addition to a blank with no adsorbent was run. The results showed that there are no significant adsorption in blank tubes.

2.4. Analytical methods

All measurements were conducted according to standard methods. The influent and effluent concentrations of metals ions were measured using the atomic absorption spectrophotometer (Thermo Fisher–iCE 3000 series) model with air – acetylene gas and wave length of 357.9 nm in the faculty of Agriculture-Central Laboratory – Zagazig University, Egypt. Values of pH were determined by using a pH meter (AD1000). Stainless-metal sieves (Standard Sieves Dual Manufacturing Co., USA) were used to get a unique particle measurement of the adsorbent. Before and after adsorption process, the surface of the studied adsorbent was photographed using scanning electron microscope (JEOL JSM-6510LV SEM, USA). Fourier transform infrared (FTIR) spectrometer (Alpha II Bruker, Germany) was used to determine the active sites and active groups present on the surface of the UMFB.

2.5. Kinetic studies

The adsorption kinetics of heavy metal ions were studied at different time intervals to understand and predict how time can affect the mobility and retention of heavy metals. The adsorption kinetics for UMFB were checked by 2 common models using the pseudo-first-order and pseudo-second-order [18].

2.6. Adsorption isotherm models

Adsorption isotherms are vital to show how adsorbates interact with adsorbent surfaces and are also used to determine the quantity of a given pollutant adsorbed from aqueous solutions.

An adsorption isotherm is characterized by certain constants that express the surface properties and the affinity of the adsorbent towards metal adsorption. There are various adsorption isotherms models but Langmuir and Freundlich equations are the most widely used ones.

2.7. Statistical analysis

Statistical analyses of the data were carried out by SPSS-version 22.0 (IBM Corp., USA) – software for windows.

2.8. Quality control/quality assurance

Several quality control methods were used to obtain reliable data. The accuracy of the result was evaluated in terms of the repeatability of the results and the presence of any target metals in the blank solution. The accuracy of the analysis was tested by analyzing in triplicate. Both correlation coefficient (R^2) and standard error (SE) of estimates were used as an error functions analysis for linear and nonlinear models [19].

3. Results and discussion

3.1. Characterization of UMFB particles

SEM is a measure for adsorbent's surface morphology, and this can be an indicator of the surface area and its pore size. Fig. 1 shows the SEM images (magnification power 1,000×) of the adsorbent before and after of pollutants adsorption. The pre-adsorption SEM images of the UMFB particles showed an irregular shaped surface and a heterogeneous structure. This indicates that the UMFB surface has a high tendency to trap and adsorb heavy metals. As presented in Fig. 1, obvious changes of the surface were observed upon adsorption of Cd, Cu, or Pb where the roughness was replaced by a smoother surface. In general, an increase in the surface roughness leads to an increase in the surface area of adsorbent, providing more active adsorption sites for heavy metals [20]. This is in line with the high adsorption capacity (q_e) obtained for UMFB in comparison with many other adsorbents.

3.2. Sorption mechanism

FTIR is one of the most common methods for identifying different functional groups constituting a compound [21]. The IR absorption spectra of the UMFB recorded in the range of 4,000–500 cm^{-1} are shown in Fig. 2. As seen in the spectrum of UMFB, the broad and intense peak at around 3,266 cm^{-1} corresponds to hydrogen bond –OH stretching, indicating that the occurrence of alcohols and phenols are present in the structure. This finding is similar to those of Guan et al. [22] who found that the band between 3,250–3,450 cm^{-1} represents the stretching vibration of –OH and N–H groups. The C–H stretching vibrations between 2,918 and 2,850 cm^{-1} can be assigned to the aromatic ring stretching and alkanes. In a previous study, Ayub et al. [23] depicted that the peaks at 2,849 and 2,922 cm^{-1} were attributed to the stretching vibrations of $–CH_2$. The peaks

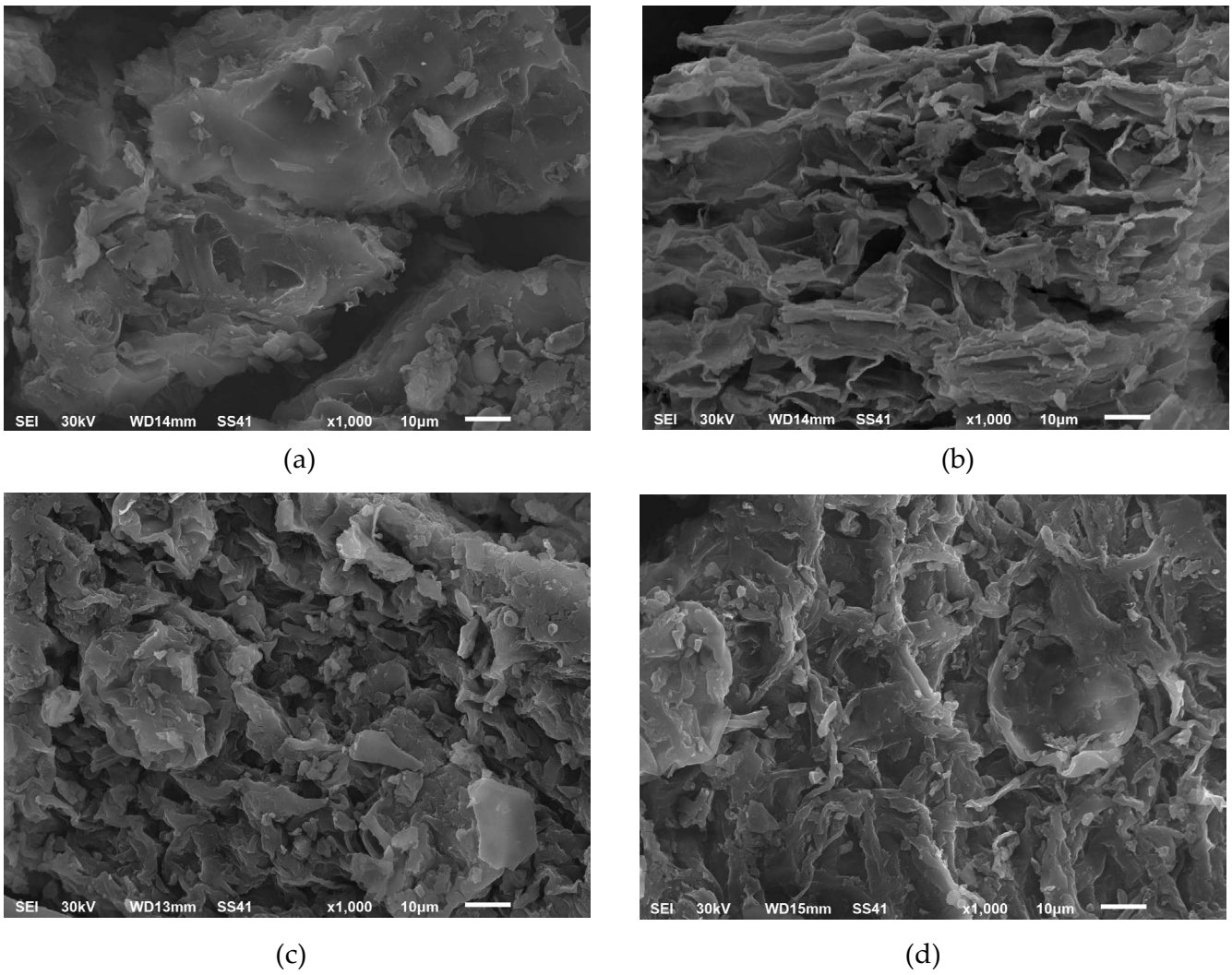

Fig. 1. SEM images of UMFB: (a) before adsorption, (b) after Cd adsorption, (c) after Cu adsorption, and (d) after Pb adsorption.

found at 1,606 and 1,315 cm^{-1} were attributed to the presence of C–O stretching [24,25]. The two tiny peaks located at 1,196 and 1,160 cm^{-1} and the sharp peak at 1,027 cm^{-1} was linked to the C–O–C stretching vibration [25]. The peak in raw UMFB was slightly shifted after metal adsorption. The results showed that UMFB conserves and generates a large amount of functional groups on its surface, which can improve its adsorptive properties.

3.3. Effect of adsorbent dosage

The adsorbent dosage effect on heavy meal biosorption was run with 1, 3, 6 and 10 g/L. Fig. 3 shows the relationship between the adsorbent dose vs. the removal efficiency and the adsorption capacity (at contact time = 60 min, pH = 5, temperature = 30°C, and agitation speed = 150 rpm).

As shown in Fig. 3, the heavy metals (Cd, Cu, Pb) removal increased gradually from 69.58% to 82.46%, from 58.89% to 65.74% and from 69.72% to 74.99%, respectively, with a rise in the adsorbent dose from 1.0 to 6.0 g/L. However, no significant elevation in Cd removal was noticed with additional elevation in adsorbent mass more than 6 g/L. A rise in the adsorbent mass from 6 to 10 g/L increased the removal efficiency from 65.74% to 73.83% for Cu and from 74.99% to 78.05% for Pb. In other words, using 3 g/L of UMFB is sufficient to adsorb more than 70% Cd and Pb having 50 mg/L initial concentration within 60 min, while 10 g/L of adsorbent is required to adsorb more than 70% Cu. Moreover, a rise in the UMFB mass from 1 to 10 g/L affected negatively the q_e (36.64–4.40 mg/g), (31.13–3.90 mg/g), (36.70–4.08 mg/g) for Cd, Cu, and Pb respectively.

Several studies that have examined the effect of increasing the adsorbent dosage on removing heavy meals have concluded that the improvement of removal efficiency is due to the increase in the surface area and accessible active sites of adsorbent available for the pollutant removal [26,27]. Also, Gupta et al. [28] attributed the reason to the presence of sorption space in which adsorbate will bind. Al-Jabari et al. [29] indicated that more particles in liquid mean that more collisions can occur with their surfaces, leading to faster adsorption. Pooresmaeil and Namazi [30] indicated that the removal efficiency is usually enhanced by increasing

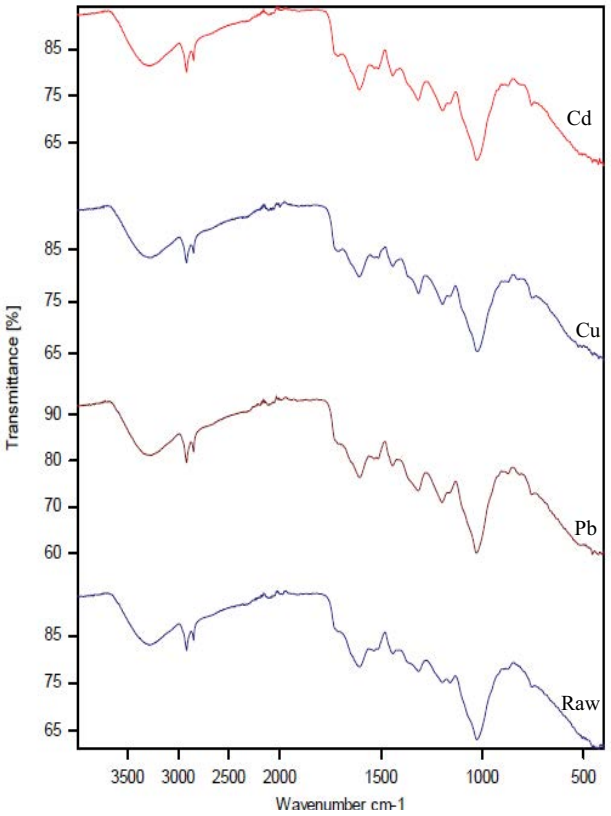

Fig. 2. FTIR spectrum of UMFB before adsorption.

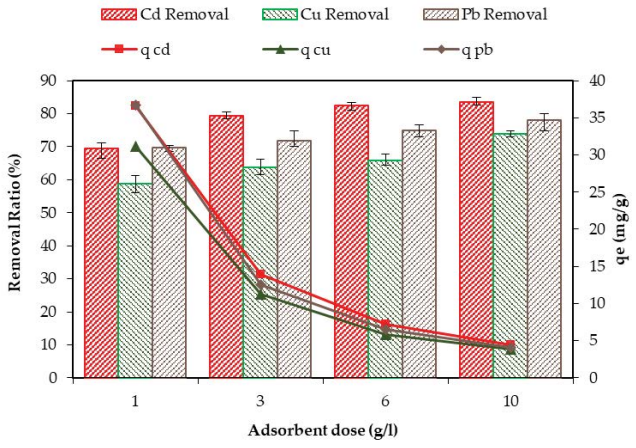

Fig. 3. Effect of the adsorbent dose on the removal efficiency and the biosorption capacity at contact time = 60 min, pH = 5, temperature = 30°C, and agitation speed = 150 rpm.

the amount of adsorbent dosage, but after reaching a certain amount, the adsorption capacity remains constant. Karaca [31] explained that there is a relation between the biomass amount and the sorption at a higher adsorbent dose due to the availability of the metal ion that might be limited with the increased electrostatic interactions, interference between binding sites, and reduced mixing. The decrease in adsorption capacity with a rise in the adsorbent mass is attributed

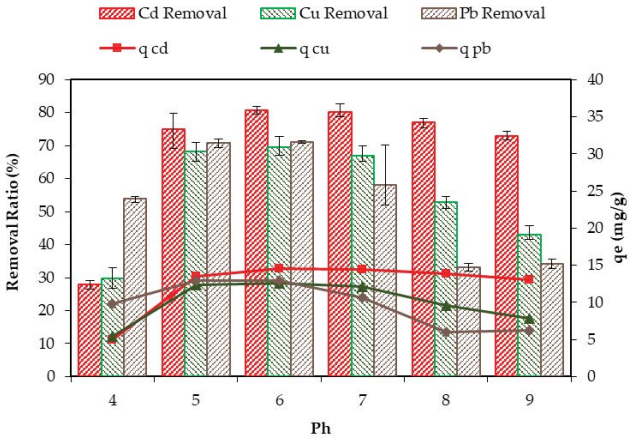

Fig. 4. Effect of pH on the removal efficiency and the adsorption capacity at an adsorbent dose = 3.0 g, contact time = 60 min, initial concentration = 50 mg/L, temperature = 30°C and agitation speed = 150 rpm.

to two reasons: (i) the adsorption sites remain unsaturated while the available adsorption pores number increase and (ii) accumulation of adsorbent particles may reduce the available surface area and increase the diffusion path length [32,33].

3.4. Effect of pH

The pH of the water has a great impact on the removal of heavy metals. The effect of pH on the removal efficiency of the different metals was investigated (at contact time = 60 min, initial concentration = 50 mg/L, temperature = 30°C and agitation speed = 150 rpm). The results shown in Fig. 4 indicated that the sorption process is a pH dependent, and the optimal sorption was observed at pH values between 5 and 6. Moreover, q_e presented a significant increase (ranging from 5.00 to 14.51 mg/g for Cd, from 5.40 to 12.57 mg/g for Cu and from 9.84 to 12.98 mg/g for Pb with an elevation in pH from 4.00 to 6.00). On the other hand, an additional elevation in pH (to 9.0) led to a decrease in q_e (to 13.07, 7.79 and 6.27 mg/g for Cd, Cu and Pb respectively). Lower adsorption at low pH (≤4) can be ascribed to excessive concentrations of H^+ ions that often interfere with the interactions of soluble metal ions and adsorbent surfaces via competing for adsorption sites and, consequently, reducing overall heavy metal removal [34,16]. While at higher pH, the presence of negatively charged functional groups as hydroxyl and oxalate ions ensures the metal oxalate complex formation, thus affecting the adsorption of metal ions on the adsorbent [35].

Various studies have examined the possible impact of pH upon heavy metal biosorption of different adsorbent materials and reported similar findings. Mustapha et al. [35] observed that maximum removal of Pb, Cd, Zn and Cu ions occurred at acidic medium and a further increase in pH above their optimum caused the formation of precipitates. Akhtar et al. [36] confirmed that the removal efficiency of Cd, Cu, Pb and Zn increased with the increase in pH up

to 6, and further increase of pH decreased the sorption. For Cd and Cu, Sha et al. [37] also found that adsorption efficiencies were relatively low at lower pH values and increased with an increase in pH with optimum values obtained at pH around 5–7. Pathak et al. [38] mentioned that the optimum pH is 5–6 while alkaline medium is inefficient for heavy metal removal.

3.5. Effect of contact time

Fig. 5 shows the relationship between contact time vs. the removal efficiency and the adsorption capacity (at an adsorbent dose = 3.0 g, pH = 5.0, initial concentration = 50 mg/L, temperature = 30°C and agitation speed = 150 rpm). As shown in Fig. 5, Cd, Cu and Pb removal increased gradually from 77.09% to 82.77%, from 66.00% to 73.26% and from 73.43% to 79.64% respectively, with an increase in contact time from 30 to 120 min. After 120 min of contact time, the relative increase in the heavy metal removal was not significant. Similarly, q_e, improved to 14.44, 12.65 and 13.07 mg/g for both Cd, Cu and Pb, respectively at 120 min. The results shown in Fig. 5 indicated that increasing the contact time from 0.5 to 2 h enhanced the percentage removal because of the large number of active sites available for adsorption and the high rate of adsorption at first. After that, the percentage removal remained constant as the active sites were about to be saturated.

This finding is supported by that of Mustapha et al. [35] who found that the percentage removal of the metal ions increased at first with increasing contact time owing to the availability of large surface areas of the adsorbent. After the maximum removal value, the desorption began due to the agglomeration of metal ions on the surface of the adsorbent. Saraswat and Rai [39] also stated that an optimum metal adsorption occurred at an agitation time of 120–180 min.

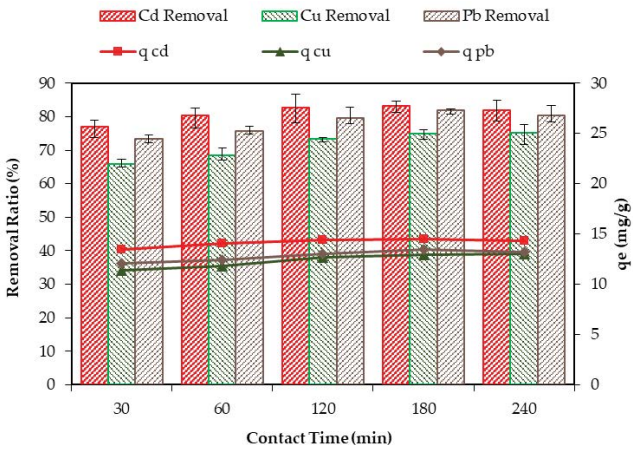

Fig. 5. Effect of the contact time on the removal efficiency and the adsorption capacity at an adsorbent dose = 3.0 g, pH = 5.0, initial concentration = 50 mg/L, temperature = 30°C and agitation speed = 150 rpm.

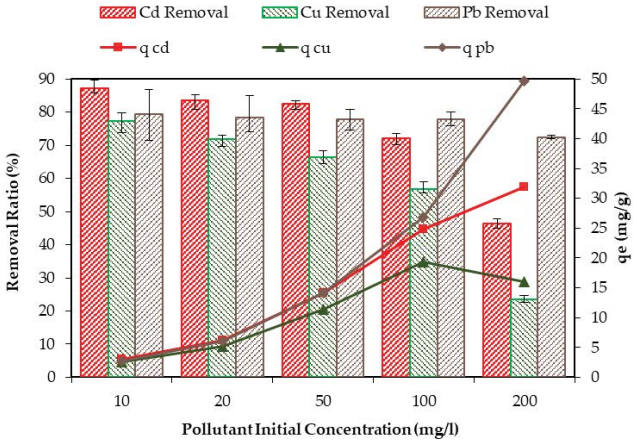

Fig. 6. Effect of the initial concentration of the pollutant on the removal efficiency and the adsorption capacity at an adsorbent dose = 3.0 g, pH = 5.0, contact time = 60 min, temperature = 30°C and agitation speed = 150 rpm.

3.6. Effect of initial concentration

The effect of initial concentration (10–200 mg/L) was studied (with pH of 5, adsorbent dosage of 3 mg/L, contact time = 60 min, temperature = 30°C and agitation speed = 150 rpm). As shown in Fig. 6, when the initial metal concentration increased from 10 to 200 mg/L, removal ratios decreased linearly. In the same time Cd removal decreased from 87.09% to 46.35%, Cu removal diminished from 77.21% to 23.41% and Pb removal declined from 79.54% to 72.41%, while q_e elevated from 2.95 to 31.85, from 2.57 to 16.05 and from 2.80 to 49.66 mg/L for Cd, Cu, and Pb respectively. In Fig. 6, the removal rate of metals from solution decreases with the increase of the initial concentration of metals, and the amount of metals adsorbed by the adsorbent increases with the increase of the initial concentration of metals in the solution. This can be interpreted by stating that increasing initial concentration of metals while the adsorbent remains constant leads to a higher equilibrium concentration of metals in the solution, which contributes to a higher amount of metals adsorbed by the adsorbent. These results agree with those of Duan et al. and Adebowale et al. [40,41] who indicated that the quantity of ions challenging for the vacant active sites in adsorbent increases at high load of metals, and, therefore, there was an inadequate surface area to house the pollutant available in the solution.

3.7. Effect of temperature

Fig. 7 presents the effect of temperature (20°C, 30°C, 40°C, 50°C, and 60°C) on the removal efficiency (at an adsorbent dose = 3.0 g, pH = 5.0, contact time = 60 min, initial concentration = 50 mg/L, and agitation speed = 150 rpm). The experimental result showed that the removal percentage of Cd, Cu, and Pb enhances when the temperature increases from 20°C to 60°C. The better adsorption at higher temperature may indicate the endothermic nature of the process. The optimum

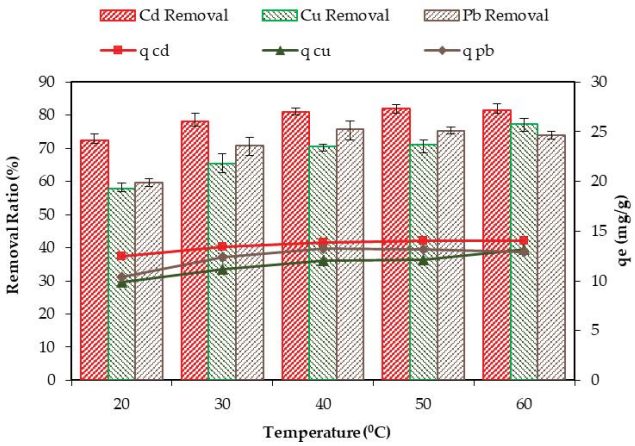

Fig. 7. Effect of the temperature on the removal efficiency and the adsorption capacity at an adsorbent dose = 3.0 g, pH = 5.0, contact time = 60 min, initial concentration = 50 mg/L and agitation speed = 150 rpm.

removal was at 40°C by 80.90% and 75.75% for Cd and Pb respectively, and at 60°C by 77.32% for Cu. Such an increase in the adsorption capacity is due to the increase of kinetic energy at higher temperature, which increases the collision frequency between solute and adsorbent. Mustapha et al. [35] asserted that the increase in adsorption of metal ions can be related to the increased mobility of metal ions as a result of the acquired energy in the system. Also, Hu et al. [42] indicated that the rise of adsorption capacity accompanied by an increase in temperature is due to the bond rupture of functional groups on the adsorbent surface which increases active adsorption sites.

3.8. Influence of coexisting ions

Different ions can exist and compete with each other for adsorption sites as commonly seen in nature. Fig. 8 shows the effects of the coexistence of Cu^{2+}, SO_4^{2-}, and COD on Cd adsorption in terms of the removal ratio of Cd.

3.8.1. Influence of Cu^{2+}

Fig. 8a shows the removal rates of Cd with different initial concentrations of Cu^{2+}. As shown in this Fig. 8a, the amount of adsorption in a single-metal solution is greater than that of the mixed metal solutions and the removal percentage of Cd is slightly reduced when the initial concentration of Cu is low. Also, it can be noticed that Cd removal decreased from 81.97% at Cu^{2+} concentration of 10 mg/L to 55.56% with the increase of Cu^{2+} concentration to 100 mg/L. A similar trend was obtained by Xie et al. [43] who studied the effect of coexisting ions on the adsorption of Cu in the silty clay. They deduced that the adsorption process is divided into two stages for a mixed Cu and Zn solution. There is a slight difference in the amount of adsorption between the single-metal and the mixed-metal solutions at a relative low concentration and the difference increases gradually as the equilibrium concentration increases. In the same context, Mustafa et al. [44] studied the cadmium adsorption behavior on goethite. They attributed the reason for the decrease in removal of Cd with the increase in Ca^{2+} concentration to the fact that the adsorption sites of the surface of ferrihydrite for Cd were occupied by Ca^{2+}.

3.8.2. Influence of SO_4^{2-}

Adsorption behavior of Cd in the presence of SO_4^{2-} shows that adsorption process is influenced by the presence of anions (SO_4^{2-}) more than cations (Cu^{2+}) as shown in Fig. 8b. The presence of 50 and 100 mg/L of SO_4^{2-} decreased the removal rate of Cd ions to 30.89% and 12.37%, respectively in comparison with 83.64% for the single-metal solution of Cd. This negative effect of SO_4^{2-} on the removal of Cd can be attributed to the intense competitive adsorption.

3.8.3. Influence of organic matter (COD)

The organic matter (COD) was controlled in the range from 0 to 250 mg/L. As shown in Fig. 8c, the removal rate of Cd declined generally with the increase of organic matter. In response to the organic matter that range from 0 to 250 mg/L, the removal ratio decreased from 83.85% for the

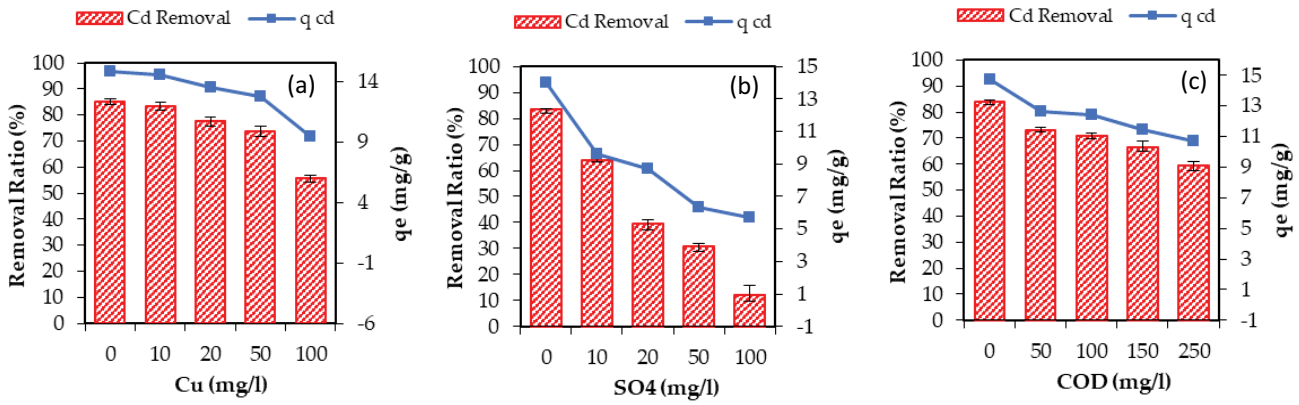

Fig. 8. Influence of coexisting ions on the removal of Cd (adsorbent dose = 3.0 g, pH = 5.0, contact time = 60 min, initial concentration Cd = 50 mg/L, and agitation speed = 150 rpm): (a) Cu, (b) SO_4^{2-}, and (c) COD.

single-metal solution of Cd to 59.62% at 250 mg/L COD concentration.

3.9. Effect of biosorption kinetics

In order to understand the kinetic behavior of the adsorption process, numerous kinetics models including the pseudo-first-order and pseudo-second-order, have been used to fit the kinetic experimental data. Tables 2 and 3 display the calculated parameters of the reaction kinetics of these models. Brief descriptions of these models are given in the following sections.

3.9.1. Pseudo-first-order kinetic model

The pseudo-first-order model assumes that the rate of change of adsorbate uptake with time is proportional to difference in adsorbate uptake at equilibrium and at any time. The kinetics follow pseudo-first-order model when adsorption occurs within diffusion through the interface [45]. The general expression for pseudo-first-order is shown in Eq. (1) while the linear form of the pseudo-first-order model can be expressed in Eq. (2):

$$\frac{dq_t}{dt} = k_1\left(q_e - q_t\right) \tag{1}$$

$$\log\left(q_e - q_t\right) = \log q_e - \frac{K_1}{2.303}t \tag{2}$$

where q_e and q_t (mg/g) represent the adsorption capacities at equilibrium and at any time (t); and K_1 is the pseudo-first-order constant (h^{-1}).

To apply the nonlinear model, the experimental data have been tested by nonlinear regression (SPSS program) while the values of q_e and K_1 in the linear form can be calculated from the slope and intercept of $\log(q_e - q_t)$ vs. time.

The experimental values of the adsorption capacities at equilibrium for Cd, Cu and Pb are 14.51, 12.61, and 9.06 mg/g respectively. These values are much higher than those predicted by linear pseudo-first-order model as shown in Table 2, and this is confirmed by the low values of the linear regression coefficients (R^2 ranging from 0.18–0.48). These values display the non-agreement of the pseudo-first-order kinetic model and the experimental data. This disagreement means that the linear form for pseudo-first-order model is not appropriate to predict the adsorption kinetics for the adsorption of Cd, Cu and Pb onto UMFB.

On the other hand, the correlation coefficients for nonlinear regression were high and the experimental values were close to the predicted values. So, the nonlinear form pseudo-first-order model can be appropriate to predict the adsorption kinetics for the adsorption of Cd, Cu and Pb onto UMFB.

3.9.2. Pseudo-second-order model

The pseudo-second-order model assumes that the reaction is inclined towards chemical sorption or chemisorption. In this model, the adsorption rate is dependent on the adsorption capacity not on the concentration of adsorbate [45]. The general expression for pseudo-second-order is shown in Eq. (3) while the linear form of the pseudo-second-order model can be expressed in Eq. (4):

$$\frac{dq_t}{dt} = k_2\left(q_e - q_t\right)^2 \tag{3}$$

$$\frac{t}{q_t} = \frac{1}{k_2 q_e^2} + \frac{1}{q_e}t \tag{4}$$

where K_2 is the rate constant of second-order adsorption and the second-order kinetic parameters, K_2 and q_e, are calculated for different metals using the slope and the intercept of the graph of the linear plot form between t/q_t vs. time while SPSS program is used to treat the experimental data for the nonlinear model.

The calculated q_e values obtained from pseudo-second-order model were in good agreement with the experimental values since the linear q_e values were 14.48, 12.01 and 9.0 mg/g and the nonlinear values were 14.63, 12.48 and 9.13 mg/g for Cd, Cu and Pb respectively, as listed in Table 3. In addition, the correlation coefficient, R^2, for the second-order kinetic model was almost equal to 1.0 for all the metals signifying the applicability of the model in both forms. Thus, it appeared that the system under study is more suitably described by pseudo-second-order model that is based on the assumption that the rate

Table 2
Parameters of pseudo-first-order model for Cd, Cu, and Pb

Model form	Parameters	Metal ion		
		Cd	Cu	Pb
Linear form	q_e (mg/g)	0.95	1.25	0.73
	K_1 (h^{-1})	0.37	0.26	0.41
	R^2	0.48	0.18	0.42
Nonlinear form	q_e (mg/g)	14.34	12.14	8.90
	K_1 (h^{-1})	5.47	4.58	4.88
	R^2	0.86	0.68	0.87

Table 3
Parameters of pseudo-second-order model for Cd, Cu, and Pb

Model form	Parameters	Metal ion		
		Cd	Cu	Pb
Linear form	q_e (mg/g)	14.48	12.01	9.00
	K_2 (h^{-1})	2.72	34.45	3.54
	R^2	0.99	0.99	0.99
	SE	0.24	0.79	0.22
Nonlinear form	q_e (mg/g)	14.63	12.48	9.13
	K_2 (h^{-1})	1.58	1.25	1.89
	R^2	0.99	0.97	0.99
	SE	0.14	0.44	0.13

limiting step may be chemisorptions concerning forces of valances through sharing and exchanging of electrons.

3.10. Adsorption isotherm studies

3.10.1. Langmuir model

Langmuir model is a theoretical model based on the following assumptions: (i) adsorbent's surface is homogenous and flat; (ii) the adsorbate forms a single monolayer; and (iii) no interaction occurs between the adsorbed molecules [46]. The Langmuir model is reported in Eq. (5) while the linear form of Langmuir isotherm is shown in Eq. (6):

$$q_e = \frac{q_m C_e b}{1 + C_e b} \tag{5}$$

$$\frac{C_e}{q_e} = \frac{C_e}{q_m} + \frac{1}{q_m b} \tag{6}$$

where q_e is the adsorption capacity of adsorbent at equilibrium (mg/g), q_m is the maximum adsorption capacity (mg/g), b is the Langmuir's adsorption constant (L/mg) and C_e is the equilibrium concentration in the liquid phase (mg/L). The material effectiveness is shown by q_m while b belongs to the sympathy of metals to the adsorbent surface.

For Eq. (5), the values of q_m and b can be obtained by nonlinear regression (SPSS program). For the linear form in Eq. (6), the values of q_m and b can be obtained from the slope and the intercept of the linear plot of C_e/q_e vs. C_e.

The Langmuir equation can be expressed in terms of a dimensionless constant, R_L, which is given as:

$$R_L = \frac{1}{1 + C_0 b} \tag{7}$$

where C_0 is the initial metal concentration (mg/L) and R_L is the equilibrium parameter which indicates that the adsorption possibility can be favorable ($0 < R_L < 1$), unfavorable ($R_L > 1$), linear ($R_L = 1$) or irreversible ($R_L = 0$).

Table 4 describes the values of Langmuir model parameters (linear form and nonlinear form) for the adsorptions of studied metal ions on UMFB. The q_m and b values for the linear form were about (37.13, 0.063), (16.89, 0.119) and (155, 0.008) mg/g and L/mg, for Cd, Cu and Pb. The q_m and b values for the nonlinear form were about (37.17, 0.068), (19.37, 0.085) and (137.86, 0.01) mg/g and L/mg, for Cd, Cu and Pb. on the other hand, Pb and Cu did not respond well to the linear and nonlinear forms respectively as confirmed by values of linear regression coefficient (R^2 = 0.91) for Pb and nonlinear regression coefficient (R^2 = 0.89) for Cu. The R_L values shown in Table 4 reveal that biosorption of Cd and Cu were more favorable than Pb biosorption.

3.10.2. Freundlich model

The Freundlich model is considered an empirical equation supposing that the adsorption of metal ions takes place on a heterogeneous surface by multilayer adsorption [27]. The model of the Freundlich isotherm is reported in Eq. (8), while the linear form of Freundlich isotherm is shown in Eq. (9):

$$q_e = k_f C_e^{\frac{1}{n}} \tag{8}$$

$$\ln q_e = \ln k_f + \frac{1}{n} \ln C_e \tag{9}$$

where q_e is the adsorption capacity of adsorbent at equilibrium (mg/g), k_f is the Freundlich constant ($mg^{(1-n)}/L^n$ g), C_e is the equilibrium concentration (mg/L), and $1/n$ is the heterogeneity factor. The heterogeneity factor $1/n$ is related to the capacity and intensity of the adsorption. A smaller $1/n$ value indicates a more heterogeneous surface. An n value between 1 and 10 indicates a high adsorption capacity and values less than 1.0 indicate a small adsorption capacity [27,47,48]. For Eq. (8), the values of k_f and n can be obtained by nonlinear regression (SPSS program). For the linear form in Eq. (9), the values of k_f and $1/n$ can be obtained from the slope and the intercept of the plot of $\ln q_e$ against $\ln C_e$.

As listed in Table 5, the values of k_f and n for Freundlich's linear form were (3.01, 1.76), (2.29, 2.17) and (1.46, 1.12) for Cd, Cu and Pb respectively. The k_f and n values for Freundlich's nonlinear form were (5.52,2.56), (4.44, 3.52), (1.97, 1.25) for Cd, Cu and Pb respectively. The n was above 1.00, indicating that the biosorption of Cd, Cu and Pb on UMFB was favorable at the studied conditions.

Values of R^2 indicate that only Pb respond well to Freundlich's linear and nonlinear forms.

The results show that the adsorption of Cd, Cu, and Pb fits the Langmuir model better than the Freundlich model. The fact that the Langmuir model is a good fit to the experimental results suggests a homogeneous distribution of active sites on the UMFB, which is consistent with Langmuir model's assumption.

3.11. Comparison with others materials

The adsorption capacity of different types of materials (Cd, Cu and Pb) has been compared with those of others

Table 4
Parameters of Langmuir isotherm model for Cd, Cu, and Pb

Model form	Parameters	Metal ion		
		Cd	Cu	Pb
Linear form	q_e (mg/g)	37.13	16.89	155
	b (L/mg)	0.063	0.119	0.0084
	R_L	0.29	0.20	0.68
	R^2	0.99	0.98	0.91
	SE	1.19	3.03	1.01
Nonlinear form	q_e (mg/g)	37.17	19.37	137.86
	b (L/mg)	0.068	0.085	0.01
	R_L	0.28	0.25	0.65
	R^2	0.99	0.89	0.99
	SE	1.04	2.65	0.88

reported in previous studies and the values of adsorption capacity are presented in Table 6. Results of the current study revealed that UMFB surface has a very good adsorption capacity. UMFB has significant advantages compared to other adsorbents. When compared to different adsorbents materials, UMFB is a good alternative for Cd, Cu and Pb removal. This emphasizes the importance of finding locally accessible materials with a high pollutant maintenance limit for the purpose of utilization in heavy metal removal. UMFB is novel low-costs adsorbents, representing a promising green technology since the outcomes reveal that the adsorption of concerned pollutants on raw UMFB is optimistic. From the perspective of material accessibility, it is considered a suitable material amongst the most adequate feedstock regarding the approval included item because it is adaptable to different environmental conditions, easy to harvest and highly rich in biomass. The utilization of UMFB has been limited because of insufficient studies showing its ability to remove heavy metals. Financial and natural point of view is highly considered when selecting the simple methodological tools and materials in the present study. For example, making of dried UMFB powder costs much less money in comparison with other methods requiring some sort of preparation of different materials with changes and additives that cost a lot of money in addition to the ecological unsafe added substances (chemicals/reagents). In fact, the only chemical used in this study to get the UMFB powder is HCL (1 N) and NaOH.

4. Conclusions

Removal of heavy metals is one of the most crucial problems at present, and such problems arise as a result of environmental pollution, springing from industrialization and urbanization. Traditional treatment techniques are ineffective in the removing process. For all these reasons, further research in the field of heavy metal adsorption and environmental protection should be focused on modifications and characterizations of all available waste sources, including agro-based adsorbents that can protect water sources and the environment. In this work, the potentials of a new possible adsorbent (UMFB) for purifying water from metal ions have been traced. The present study has showed that UMFB powder can be used as a natural, promising, economic and environmentally friendly adsorbent for removing Cd, Cu, and Pb from aqueous solutions. The studies of SEM showed that surface morphology on UMFB before adsorption was an irregular heterogeneous structure, which became flattened after the adsorption process. There was shifting of bands in the FTIR spectrum of UMFB, confirming that the heavy metals (Cd, Cu, Pb) were being adsorbed on UMFB. The batch experiments show that the adsorbent dosage, initial pH, contact time, initial metal concentration and temperature had a great impact on adsorption properties. The increased concentration of adsorbent and temperature values enhanced the removal process and the increased initial pollutant concentration reduced it. The study of adsorption of Cd, Cu, and Pb in aqueous solutions at pH values in the range of 4.0–9.0 and contact time from 30–240 min showed that the adsorption rate was the best at 6.0 pH and 120 min. The coexisting ions, such as Cu, SO_4, and organic matter, had a certain effect on the treatment since the removal efficiency of Cd ions weakened when coexisting ions increased. Kinetic studies indicate that the adsorption of Cd, Cu, and Pb on UMFB follows the pseudo-second-order due to its q_e: calculated values are closer to the q_e experimental value with a higher R^2. Both Langmuir and Freundlich models were used to fit the data to estimated model parameters, but the adsorption kinetics isotherm is better fitted by Langmuir isotherm.

The present work can be extended to further studies. The future scope has to be concerned with the effect of size of particles on the removal of heavy metal ions. In this context fixed-bed column studies under various experimental

Table 5
Parameters of Freundlich isotherm model for Cd, Cu, and Pb

Model form	Parameters	Metal ion		
		Cd	Cu	Pb
Linear form	k_f (mg/g)	3.01	2.29	1.46
	n (L/mg)	1.76	2.17	1.12
	R^2	0.92	0.84	0.99
	SE	7.42	5.81	2.75
Nonlinear form	k_f (mg/g)	5.52	4.44	1.97
	n (L/mg)	2.56	3.52	1.25
	R^2	0.91	0.68	0.99
	SE	4.21	4.46	1.68

Table 6
A comparison of adsorption capacity of different adsorbents for the adsorption of Cd, Cu, and Pb

Pollutant	Adsorbents	Adsorbent capacity (mg/g)	References
Cd	Corncob	5.1	[49]
	Orange peel	41.8	[50]
	Banana peel	34.1	[50]
	Grapefruit peel	42.1	[51]
	UMFB	36.64	This work
Cu	Rice straw	18.4	[52]
	Rice husks	17.9	[52]
	Peanut shells	25.4	[53]
	Peanut husks	10.2	[54]
	Groundnut shells	4.9	[55]
	Banana peel	38.3	[56]
	Grape stalk	10.1	[57]
	UMFB	31.13	This work
Pb	Corncob	16.2	[58]
	Peanut husks	29.1	[54]
	Lemon peel	37.9	[50]
	Orange peel	27.1	[50]
	Orange peel	27.9	[59]
	Banana peel	7.9	[60]
	UMFB	49.66	This work

conditions have to be conducted. In addition, structural and textural parameters that are used for the characterization of metal ions adsorption can provide further clarifications for a comprehensive understanding of the mechanism of the reaction between heavy metals and the UMFB.

Acknowledgement

The authors express gratitude to the staff of employees of Environmental Engineering Laboratory – Faculty of engineering – Zagazig University.

References

[1] M.J.A. Alatabe, Utilization of conventional treatments and agricultural wastes as low-cost adsorbents for removal of lead ions from wastewater, UKH J. Sci. Eng., 5 (2021) 1–17.
[2] X. Chen, H. Gao, X. Yao, Z. Chen, H. Fang, S. Ye, Ecosystem health assessment in the Pearl River Estuary of China by considering ecosystem coordination, PLoS One, 8 (2013) e70547, doi: 10.1371/journal.pone.0070547.
[3] G. Palani, A. Arputhalatha, K. Kannan, S.K. Lakkaboyana, M.M. Hanafiah, V. Kumar, R.K. Marella, Current trends in the application of nanomaterials for the removal of pollutants from industrial wastewater treatment—a review, Molecules, 26 (2021) 2799, doi: 10.3390/molecules26092799.
[4] El-Sayed E. Mehana, A.F. Khafaga, S.S. Elblehi, M.E. Abd El-Hack, M.A.E. Naiel, M. Bin-Jumah, S.I. Othman, A.A. Allam, Biomonitoring of heavy metal pollution using acanthocephalans parasite in ecosystem: an updated overview, Animals, 10 (2020) 811, doi: 10.3390/ani10050811.
[5] M. Krivokapić, Study on the evaluation of (heavy) metals in water and sediment of Skadar Lake (Montenegro), with BCF assessment and translocation ability (TA) by Trapa natans and a review of SDGs, Water, 13 (2021) 876, doi: 10.3390/w13060876.
[6] G. Jing, S. Ren, S. Pooley, W. Sun, P. Kowalczuk, Z. Gao, Electrocoagulation for industrial wastewater treatment: an updated review, Environ. Sci. Water Res. Technol., 7 (2021) 1177–1196.
[7] WHO, Guidelines for Drinking-Water Quality: Fourth Edition Incorporating the First Addendum, World Health Organization, Geneva, 2017a.
[8] WHO, Progress on Drinking Water, Sanitation and Hygiene: 2017 Update and SDG Baselines, (UNICEF), United Nations Children's Fund, 2017b.
[9] MOHP, Decree of Health Ministry (No. 458): Egyptian Standards for Drinking Water and Domestic Uses, 2007.
[10] UN-Water, The United Nations World Water Development Report 2018: Nature-Based Solutions for Water, UNESCO, Paris, France, 2018.
[11] M. de Kwaadsteniet, P.H. Dobrowsky, A. van Deventer, W. Khan, T.E. Cloete, Domestic rainwater harvesting: microbial and chemical water quality and point-of-use treatment systems, Water, Air, Soil Pollut., 224 (2013) 1629, doi: 10.1007/s11270-013-1629-7.
[12] Ihsanullah, A. Abbas, A.M. Al-Amer, T. Laoui, M.J. Al-Marri, M.S. Nasser, M. Khraisheh, M.A. Atieh, Heavy metal removal from aqueous solution by advanced carbon nanotubes: critical review of adsorption applications, Sep. Purif. Technol., 157 (2016) 141–161.
[13] S. Velusamy, A. Roy, S. Sundaram, T. Kumar Mallick, A review on heavy metal ions and containing dyes removal through graphene oxide-based adsorption strategies for textile wastewater treatment (Chem. Rec. 7/2021), The Chem. Rec., 21 (2021) 1569–1569, doi: 10.1002/tcr.202180701.
[14] G. Crini, E. Lichtfouse, L.D. Wilson, N. Morin-Crini, Conventional and non-conventional adsorbents for wastewater treatment, Environ. Chem. Lett., 17 (2018) 195–213.
[15] V. Jabbari, J.M. Veleta, M. Zarei-Chaleshtori, J. Gardea-Torresdey, D. Villagrán, Green synthesis of magnetic MOF@GO and MOF@CNT hybrid nanocomposites with high adsorption capacity towards organic pollutants, Chem. Eng. J., 304 (2016) 774–783.
[16] L. Joseph, B.-M. Jun, J.R.V. Flora, C.M. Park, Y. Yoon, Removal of heavy metals from water sources in the developing world using low-cost materials: a review, Chemosphere, 229 (2019) 142–159.
[17] E. Meez, A. Rahdar, G.Z. Kyzas, Sawdust for the removal of heavy metals from water: a review, Molecules, 26 (2021) 4318, doi: 10.3390/molecules26144318.
[18] E. Pretsch, P. Bühlmann, M. Badertscher, Structure Determination of Organic Compounds, Springer, Berlin, Heidelberg, 2009.
[19] G. Kutralam-Muniasamy, F. Pérez-Guevara, I. Elizalde Martínez, V. Shruti, Overview of microplastics pollution with heavy metals: analytical methods, occurrence, transfer risks and call for standardization, J. Hazard. Mater., 415 (2021) 125755, doi: 10.1016/j.jhazmat.2021.125755.
[20] L.B.L. Lim, N. Priyantha, Y.C. Lu, N.A.H. Mohamad Zaidi, Adsorption of heavy metal lead using *Citrus grandis* (Pomelo) leaves as low-cost adsorbent, Desal. Water Treat., 166 (2019) 44–52.
[21] V. Hospodarova, E. Singovszka, N. Stevulova, Characterization of cellulosic fibers by FTIR spectroscopy for their further implementation to building materials, Am. J. Anal. Chem., 9 (2018) 303–310.
[22] Y. Guan, H. Su, C. Yang, L. Wu, S. Chen, J. Gu, W. Zhang, D. Zhang, Ordering of hollow Ag-Au nanospheres with butterfly wings as a bio-template, Sci. Rep., 8 (2018) 9261, doi: 10.1038/s41598-018-27679-5.
[23] A. Ayub, Z.A. Raza, M.I. Majeed, M.R. Tariq, A. Irfan, Development of sustainable magnetic chitosan biosorbent beads for kinetic remediation of arsenic contaminated water, Int. J. Biol. Macromol., 163 (2020) 603–617.
[24] A. El Shahawy, G. Heikal, Organic pollutants removal from oily wastewater using clean technology economically, friendly biosorbent (*Phragmites australis*), Ecol. Eng., 122 (2018) 207–218.
[25] R. Md Salim, J. Asik, M.S. Sarjadi, Chemical functional groups of extractives, cellulose and lignin extracted from native *Leucaena leucocephala* bark, Wood Sci. Technol., 55 (2021) 295–313.
[26] Y. Kuang, X. Zhang, S. Zhou, Adsorption of methylene blue in water onto activated carbon by surfactant modification, Water, 12 (2020) 587, doi: 10.3390/w12020587.
[27] U.A. Edet, A.O. Ifelebuegu, Kinetics, isotherms, and thermodynamic modeling of the adsorption of phosphates from model wastewater using recycled brick waste, Processes, 8 (2020) 665, doi: 10.3390/pr8060665.
[28] A. Gupta, V. Sharma, K. Sharma, V. Kumar, S. Choudhary, P. Mankotia, B. Kumar, H. Mishra, A. Moulick, A. Ekielski, P.K. Mishra, A review of adsorbents for heavy metal decontamination: growing approach to wastewater treatment, Materials, 14 (2021) 4702, doi: 10.3390/ma14164702.
[29] M. Al-Jabari, H. Dwiek, N. Zahdeh, N. Eqefan, Reducing organic pollution of wastewater from milk processing industry by adsorption on marlstone particles, Int. J. Therm. Environ. Eng., 15 (2017) 57–61.
[30] M. Pooresmaeil, H. Namazi, Application of Polysaccharide-Based Hydrogels for Water Treatments, Y. Chen, Ed., Hydrogels Based on Natural Polymers, Elsevier, Amsterdam, 2020, pp. 411–455.
[31] M. Karaca, Biosorption of Aqueous Pb^{2+}, Cd^{2+}, and Ni^{2+} Ions by *Dunaliella salina*, *Oocystis* sp., *Porphyridium cruentum*, and *Scenedesmus protuberans* Prior to Atomic Spectrometric Determination, M.Sc. Thesis in Chemistry, Graduate School of Engineering and Sciences of İzmir Institute of Technology, 2008.
[32] S. Shakoor, A. Nasar, Removal of methylene blue dye from artificially contaminated water using citrus limetta peel waste as a very low cost adsorbent, J. Taiwan Inst. Chem. Eng., 66 (2016) 154–163.
[33] K.Y. Hor, J.M.C. Chee, M.N. Chong, B. Jin, C. Saint, P.E. Poh, R. Aryal, Evaluation of physicochemical methods in enhancing the adsorption performance of natural zeolite as low-cost

adsorbent of methylene blue dye from wastewater, J. Cleaner Prod., 118 (2016) 197–209.
[34] X. Li, D. Zhang, F. Sheng, H. Qing, Adsorption characteristics of Copper(II), Zinc(II) and Mercury(II) by four kinds of immobilized fungi residues, Ecotoxicol. Environ. Saf., 147 (2018) 357–366.
[35] S. Mustapha, D.T. Shuaib, M.M. Ndamitso, M.B. Etsuyankpa, A. Sumaila, U.M. Mohammed, M.B. Nasirudeen, Adsorption isotherm, kinetic and thermodynamic studies for the removal of Pb(II), Cd(II), Zn(II) and Cu(II) ions from aqueous solutions using *Albizia lebbeck* pods, Appl. Water Sci., 9 (2019) 142, doi: 10.1007/s13201-019-1021-x.
[36] M. Akhtar, S. Iqbal, A. Kausar, M.I. Bhanger, M.A. Shaheen, An economically viable method for the removal of selected divalent metal ions from aqueous solutions using activated rice husk, Colloids Surf., B, 75 (2010) 149–155.
[37] S. Liang, X. Guo, N. Feng, Q. Tian, Adsorption of Cu^{2+} and Cd^{2+} from aqueous solution by mercapto-acetic acid modified orange peel, Colloids Surf., B, 73 (2009) 10–14.
[38] P.D. Pathak, S.A. Mandavgane, B.D. Kulkarni, Fruit peel waste as a novel low-cost bio adsorbent, Rev. Chem. Eng., 31 (2015), doi: 10.1515/revce-2014-0041.
[39] S. Saraswat, J.P.N. Rai, Heavy metal adsorption from aqueous solution using *Eichhornia crassipes* dead biomass, Int. J. Miner. Process., 94 (2010) 203–206.
[40] P. Duan, C. Yan, W. Zhou, D. Ren, Development of fly ash and iron ore tailing based porous geopolymer for removal of Cu(II) from wastewater, Ceram. Int., 42 (2016) 13507–13518.
[41] K.O. Adebowale, I.E. Unuabonah, B.I. Olu-Owolabi, The effect of some operating variables on the adsorption of lead and cadmium ions on kaolinite clay, J. Hazard. Mater., 134 (2006) 130–139.
[42] Z. Hu, L. Lei, Y. Li, Y. Ni, Chromium adsorption on high-performance activated carbons from aqueous solution, Sep. Purif. Technol., 31 (2003) 13–18.
[43] S. Xie, Z. Wen, H. Zhan, M. Jin, An experimental study on the adsorption and desorption of Cu(II) in silty clay, Geofluids, 2018 (2018) 1–12, doi: 10.1155/2018/3610921.
[44] G. Mustafa, B. Singh, R.S. Kookana, Cadmium adsorption and desorption behaviour on goethite at low equilibrium concentrations: effects of pH and index cations, Chemosphere, 57 (2004) 1325–1333.
[45] T.R. Sahoo, B. Prelot, Chapter 7 – Adsorption Processes for the Removal of Contaminants From Wastewater: The Perspective Role of Nanomaterials and Nanotechnology, B. Bonelli, F. Freyria, I. Rossetti, R. Sethi, Eds., Nanomaterials for the Detection and Removal of Wastewater Pollutants, Elsevier, 2020, pp. 161–222.
[46] J.R. Guarín Romero, J.C. Moreno-Piraján, L. Giraldo Gutierrez, Kinetic and equilibrium study of the adsorption of CO_2 in ultramicropores of resorcinol-formaldehyde aerogels obtained in acidic and basic medium, J. Carbon Res., 4 (2018) 52, doi: 10.3390/c4040052.
[47] M. Brdar, M. Šćiban, A. Takači, T. Došenović, Comparison of two and three parameters adsorption isotherm for Cr(VI) onto Kraft lignin, Chem. Eng. J., 183 (2012) 108–111.
[48] M. Rahim, M.R.H. Mas Haris, Chromium(VI) removal from neutral aqueous media using banana trunk fibers (BTF)-reinforced chitosan-based film, in comparison with BTF, chitosan, chitin and activated carbon, SN Appl. Sci., 1 (2019), doi: 10.1007/s42452-019-1206-9.
[49] R. Leyva-Ramos, L. Bernal-Jacome, I. Acosta-Rodriguez, Adsorption of cadmium(II) from aqueous solution on natural and oxidized corncob, Sep. Purif. Technol., 45 (2005) 41–49.
[50] M. Thirumavalavan, Y.-L. Lai, L.-C. Lin, J.-F. Lee, Cellulose-based native and surface modified fruit peels for the adsorption of heavy metal ions from aqueous solution: Langmuir adsorption isotherms, J. Chem. & Eng. Data, 55 (2010) 1186–1192.
[51] M. Torab-Mostaedi, M. Asadollahzadeh, A. Hemmati, A. Khosravi, Equilibrium, kinetic, and thermodynamic studies for biosorption of cadmium and nickel on grapefruit peel, J. Taiwan Inst. Chem. Eng., 44 (2013) 295–302.
[52] B. Singha, S.K. Das, Adsorptive removal of Cu(II) from aqueous solution and industrial effluent using natural/agricultural wastes, Colloids Surf., B, 107 (2013) 97–106.
[53] A. Witek-Krowiak, R.G. Szafran, S. Modelski, Biosorption of heavy metals from aqueous solutions onto peanut shell as a low-cost biosorbent, Desalination, 265 (2011) 126–134.
[54] Q. Li, J. Zhai, W. Zhang, M. Wang, J. Zhou, Kinetic studies of adsorption of Pb(II), Cr(III) and Cu(II) from aqueous solution by sawdust and modified peanut husk, J. Hazard. Mater., 141 (2007) 163–167.
[55] S.R. Shukla, R.S. Pai, Adsorption of Cu(II), Ni(II) and Zn(II) on dye loaded groundnut shells and sawdust, Sep. Purif. Technol., 43 (2005) 1–8.
[56] B. DeMessie, E. Sahle-Demessie, G.A. Sorial, Cleaning water contaminated with heavy metal ions using pyrolyzed biochar adsorbents, Sep. Sci. Technol., 50 (2015) 2448–2457.
[57] I. Villaescusa, N. Fiol, M. Martínez, N. Miralles, J. Poch, J. Serarols, Removal of copper and nickel ions from aqueous solutions by grape stalks wastes, Water Res., 38 (2004) 992–1002.
[58] G. Tan, H. Yuan, Y. Liu, D. Xiao, Removal of lead from aqueous solution with native and chemically modified corncobs, J. Hazard. Mater., 174 (2010) 740–745.
[59] A.A. Abdelhafez, J. Li, Removal of Pb(II) from aqueous solution by using biochars derived from sugar cane bagasse and orange peel, J. Taiwan Inst. Chem. Eng., 61 (2016) 367–375.
[60] G. Annadurai, R.S. Juang, D.J. Lee, Adsorption of heavy metals from water using banana and orange peels, Water Sci. Technol., 47 (2003) 185–190.